The Epithelial–Stromal Microenvironment in Early Colonic Neoplasia

Takayasu Ideta[1], Boyang Li[2], Christopher Flynn[3], Yuichi Igarashi[1], Geoffrey Lowman[4], Tim Looney[4], Thomas J. Devers[5], John Birk[5], Faripour Forouhar[6], Charles Giardina[2], and Daniel W. Rosenberg[1]

ABSTRACT

Stromal cells play a central role in promoting the progression of colorectal cancer. Here, we analyze molecular changes within the epithelial and stromal compartments of dysplastic aberrant crypt foci (ACF) formed in the ascending colon, where rapidly developing interval cancers occur. We found strong activation of numerous neutrophil/monocyte chemokines, consistent with localized inflammation. The data also indicated a decrease in interferon signaling and cell-based immunity. The immune checkpoint and T-cell exhaustion gene *PDCD1* was one of the most significantly upregulated genes, which was accompanied by a decrease in cytotoxic T-cell effector gene expression. In addition, *CDKN2A* expression was strongly upregulated in the stroma and downregulated in the epithelium, consistent with diverse changes in senescence-associated signaling on the two tissue compartments.

Implications: Decreased CD8 T-cell infiltration within proximal colon ACF occurs within the context of a robust inflammatory response and potential stromal cell senescence, thus providing new insight into potential promotional drivers for tumors in the proximal colon.

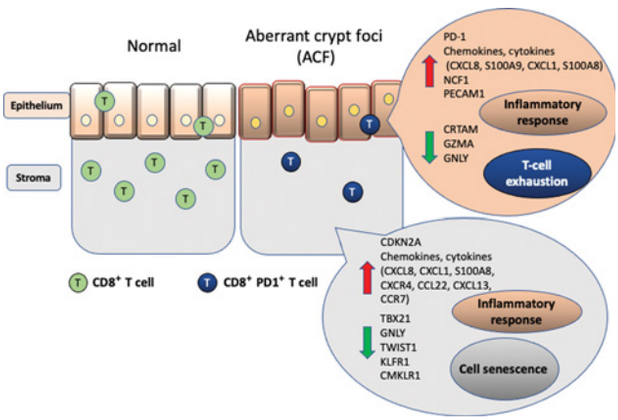

Introduction

Aberrant crypt foci (ACF) are the earliest morphologically identifiable precancerous lesion in the human colon (1–4). ACF are typically less than 5-mm in diameter and require high-definition, magnifying chromoendoscopy using contrast-dye enhancement for detection (1–5). We have reported that a significant fraction of these early neoplastic lesions harbor a range of somatic mutations within key colon cancer-related genes, including *APC*, *KRAS*, and *BRAF* (1–3). We have further shown that ACF are not uniformly distributed throughout the human colon, with the majority of ACF found within the distal colorectum (5, 6). However, those ACF identified in the proximal colon tend to display histologic features of dysplasia, often harboring significant somatic mutations to *APC*, suggesting that they are at higher risk of progression (3, 7).

We have previously reported an impressive array of stromal changes that accompany the presence of ACF (1). Among the most significant changes observed was an increase in the expression of genes related to immune cell infiltration and fibroblast activation (1). These findings indicate that immunologic pathways are altered even at the earliest stages of colonic neoplasia, which are likely to impact their neoplastic potential. A comprehensive understanding of the reaction of the host immune system to early neoplasia is important in developing new strategies for colon cancer prevention. In the current study, we expand upon our earlier targeted expression profiling of distal colorectal ACF to more deeply explore immunologic changes that accompany early colonic neoplasia in the proximal colon, where lesions can rapidly advance to interval cancers. This study provides a broad perspective on the potential role of the immune system in early neoplasia, uncovering a panel of risk markers of advanced neoplasia that we anticipate will enable a more accurate risk stratification of these early lesions.

Materials and Methods

Demographics and clinical specimens

Colon specimens were collected from 10 patients who were enrolled in a retrospective ACF study at the John Dempsey Hospital located at the UConn Health Center (Farmington, CT). Colon biopsies were immediately frozen in tissue freezing medium (OCT) on dry-ice during the colonoscopy procedure and stored at −80°C until analysis. The distal 20-cm of the colorectum and the entire proximal colon were examined endoscopically by high-definition chromoendoscopy using 0.1% indigo carmine dye-spray for contrast enhancement. We have

[1]Center for Molecular Oncology, University of Connecticut School of Medicine, Farmington, Connecticut. [2]Molecular and Cell Biology, University of Connecticut, Storrs, Connecticut. [3]Department of Pathology and Laboratory Medicine, University of Wisconsin School of Medicine and Public Health, Madison, Wisconsin. [4]ThermoFisher Scientific, South San Francisco, California. [5]Division of Gastroenterology, The University of Connecticut Health Center, Farmington, Connecticut. [6]Department of Anatomic Pathology, John Dempsey Hospital, The University of Connecticut Health Center, Farmington, Connecticut.

Note: Supplementary data for this article are available at Molecular Cancer Research Online (http://mcr.aacrjournals.org/).

T. Ideta and B. Li contributed equally to this article.

Corresponding Author: Daniel W. Rosenberg, Center for Molecular Oncology, University of Connecticut School of Medicine, 263 Farmington Avenue, Farmington, CT 06030-3101. Phone: 860-679-8704; E-mail: rosenberg@uchc.edu

Mol Cancer Res 2022;20:56–61

doi: 10.1158/1541-7786.MCR-21-0202

described the identification and histologic evaluation of ACF in our previous studies (5). In addition, each subject had a histologically confirmed corresponding normal biopsy specimen removed from the same side of the colon, generally within 2-cm of the ACF biopsy (1). The study was approved by the UConn Health Center IRB (#IE-10–068SJ-3.2) in accordance with NIH human research study guidelines.

Laser capture microdissection and RNA extraction

Highly enriched epithelial and stromal RNA samples were obtained by laser capture microdissection (LCM) using an ArcturusXT (Thermo Fisher Scientific; ref. 1). ProtectRNA RNase Inhibitor (Sigma-Aldrich) was added to each wash solution to prevent RNA degradation. Serial sections were laser captured following the manufacturer's protocol.

Ion personal genome sequencing

RNA was extracted using the Arcturus PicoPure Frozen RNA Isolation Kit and quantified using a Qubit 3.0 Fluorimeter. The quality of a subset of RNA samples was tested using a 2100 Bioanalyzer (Agilent Technologies). Reverse transcription was carried out using the SuperScript VILO cDNA Synthesis Kit (Thermo Fisher Scientific). Resultant cDNA was amplified using the Oncomine Immune Response Research Assay (Thermo Fisher Scientific) that profiles 395 immune-related RNA targets. Final libraries were quantified by qPCR and then diluted and pooled with 40 individual samples per pool. Each pool was templated using the automated Ion Chef platform using the Ion 540 Chef Kit and sequenced on the Ion S5XL sequencer using the Ion 540 chip (Thermo Fisher Scientific) at an average depth of 2 to 3 M reads per sample. A Torrent Suite plug-in "ImmuneResponseRNA" was used to convert sequence read data to expression counts for downstream data analysis. The replicates were taken from the same RNA extraction and sequenced, separately. In addition to initial quality control (QC) provided by Thermo Fisher Scientific, we analyzed the distribution of mapped reads and target detection rate for each sample, with no outliers detected. Therefore, all samples were kept for downstream analyses.

Immunofluorescence staining

Frozen sections (5 μm thick) were stained for immunofluorescence analysis of selected protein targets. We used the following primary antibodies: rabbit antibody to CD8 alpha (Monoclonal; Novus biologicals; NBP1–79055: 1:100) and mouse antibody to PD-1 (Monoclonal; Abcam; ab52587; 1:100). Images were captured using a Zeiss LSM 880 at 20× magnification and analyzed using the ImageJ-Fiji software programs. The numbers of CD8 and PD-1 dual-positive cells were counted per 200 epithelial cells.

Data analysis

Data analysis was based on the expression counts generated from the OIRRA. Differential Gene Expression (DGE) analysis and was performed using the R-package DESeq2 (version 1.26.0) in R (3.6.3; ref. 8). Samples were divided into an epithelial set and a stromal set, then DGE applied to the expression matrix of each set. Especially, results were extracted for both epithelial ACF versus normal mucosa and stromal ACF versus normal mucosa. *P* values were determined by a Wald test and then corrected for multiple testing using built-in functions from DESeq2. Genes with a fold change (FC) >1.5 or <0.67 and adjusted *P* values <0.05 were considered differentially expressed. Genes with a low detection rate (<50% in upregulated samples) were manually inspected and removed from the analysis. Principal component analysis (PCA) was performed on a normalized count matrix using variance-stabilizing transformation from DESeq2, with the top 50 variable genes. PCA plots were developed on a pooled matrix with all samples, and a matrix with only epithelial/stromal samples. Gene set analysis was performed using GeneAnalytics (https://ga.genecards.org/) to explore enriched Gene Ontology (GO) terms from both differentially upregulated and down regulated genes. Because the tested gene panels were heavily focused on immune-related genes, common GO: Biological Processes (GO:BP) were removed, including "immune response," "immune system process," "regulation of immune response," "adaptive immune response," and "innate immune response." Only results with high quality GO term scores were used ($P < 0.0001$).

Results

Patient demographics

All participants in this study had at least one dysplastic proximal ACF and were on average 57 years old, male, non-Hispanic white and moderately overweight (Supplementary Table S1). All patients had at least one polyp detected during the colonoscopy, with an average of 2.2 polyps per colon and an average of 17.6 total ACF that were identified in the distal colorectum and proximal colon by HD chromoendoscopy. The majority of participants came to the clinic for surveillance colonoscopy due to a personal history of high-risk polyps. In addition, 60% of participants had a family history of colorectal cancer. Three patients had proximal colon polyps detected during the procedure, which were histologically confirmed as tubular adenomas, with one patient also having a hyperplastic polyp (Supplementary Table S2). The remaining six patients had at least one left-sided polyp, histologically classified as either hyperplastic or a tubular adenoma (data not shown). In addition, we assessed microsatellite instability (MSI) status in the ACF and normal mucosa. All samples were found to be microsatellite stable (MSS) in this dataset (data not shown).

ACF epithelium and stroma samples show distinct expression profile

Our sample set consisted of 10 dysplastic ACF and 10 matched normal samples that were collected from the proximal colons. The histology and a chromoendoscopy image of a representative ACF with dysplastic features is shown in **Fig. 1A** and **B**. Frozen sections containing ACF were stained with H&E for routine histologic analysis and evaluated by a surgical pathologist who was blinded to the clinical and molecular findings. Dysplastic ACF were characterized by enlarged upper crypt regions with irregular shape, and stratified, elongated nuclei with disorganized (dysplastic) cellular appearance. The ACF were then separated by LCM into the epithelial and stromal compartments as shown in **Fig. 1C**. Samples were processed and extracted RNA was subjected to the OIRRA with 395 immune-related gene targets.

PCA was applied to the normalized expression matrix to evaluate broad transcriptional differences and concordance between replicates. Two biological replicates showed near-perfect alignment in the PCA plot (Supplementary Fig. S1A). Samples from epithelium and stroma showed a clear separation (**Fig. 1D**), although ACF and normal mucosa were not resolved on the PCA plots (Supplementary Fig. S1B and S1C). In a previous study using a different gene expression panel (4), we were able to resolve normal colonic mucosa from ACF crypts using PCA. However, in the ACF analyzed here were more variable, which may relate to differences in their underlying molecular defects (Supplementary Fig. S1C).

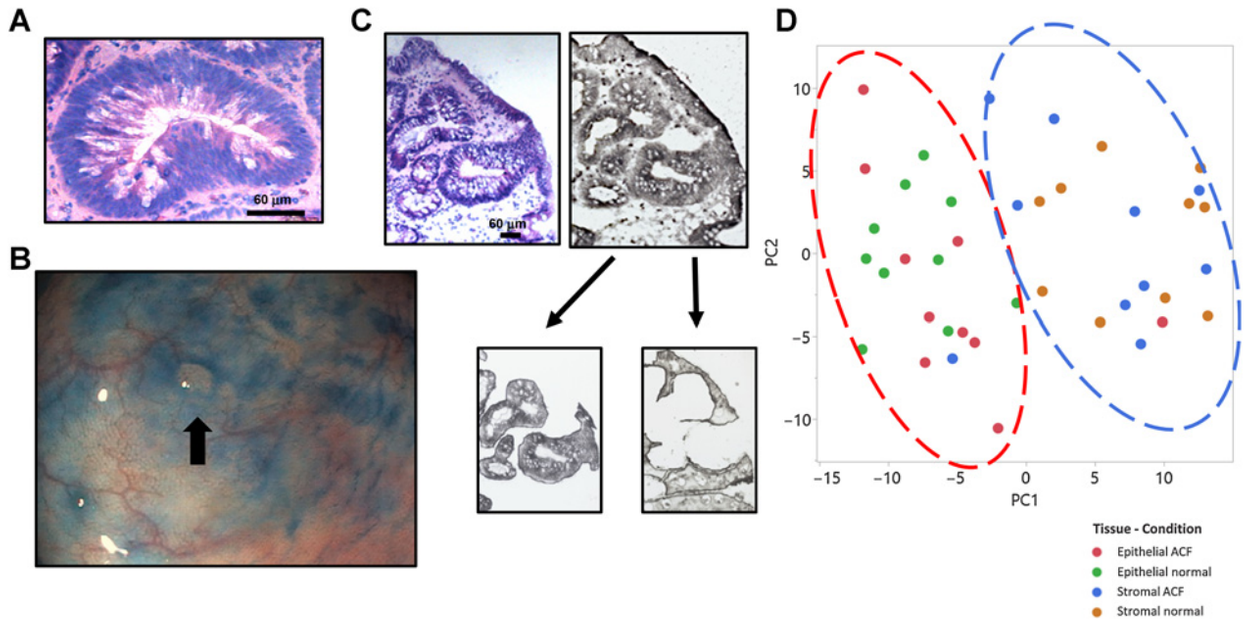

Figure 1.

Representative image of proximal dysplastic ACF and LCM capture of epithelial and stromal compartments. **A,** H&E staining of a dysplastic ACF, indicating pseudostratification and loss of goblet cells. **B,** ACF identified in the proximal colon during HD chromoendoscopy (black arrow). **C,** Hematoxylin staining of ACF (left) and unstained PEN serial section (right) of the same sample viewed from the internal camera of the Arcturus XT LCM system. Two capture groups were used: epithelial crypts (left arrow) and the surrounding stroma (right arrow). Ultraviolet laser was used to cut the tissue form the slide. Epithelial and stromal cells were captured onto separate caps for downstream RNA isolation and library preparation. **D,** PCA plot of all libraries colored by sample and condition, including the epithelial ACF samples (red), epithelial normal samples (green), stromal ACF samples (blue), and stromal normal samples (orange). Dotted lines mark clear separation between epithelial and stromal samples.

Chemokine-related genes are upregulated in the epithelial compartment of ACF

To further investigate the differences between ACF and adjacent normal mucosa, we divided all samples into an epithelial set and a stromal set and performed DGE on each set. First, we extracted significantly altered genes from the epithelial compartment. In the epithelial dataset, we identified 32 genes that were upregulated and 29 genes that were downregulated in ACF (fold change >1.5 or <0.67, adjusted $P < 0.05$; Supplementary Figs. S2A and S3). Samples from two of the patients showed outlier-like patterns, which may partially explain the lack of resolution on the PCA plots. Because of the small sample size, all samples were kept for downstream analysis, and manual curation was applied to prevent bias.

To develop a better biological understanding of the differentially expressed genes, we performed a gene set analysis using the GeneAnalytics tool (https://ga.genecards.org/) to find enriched Gene Ontology (GO) terms in each gene set. We found that many of the genes upregulated in the epithelial compartment of ACF are related to chemokine functions (GO terms "Chemotaxis," "Neutrophil Chemotaxis," "Chemokine-mediated signaling pathway," and "Chemokine production"; **Fig. 2A**). As shown in **Table 1**, five of these genes are chemokines, including *CXCL8*, *CXCL9*, *S100A9*, *CXCL1*, and *S100A8*. In addition, we found an increase in the chemokine receptor, *CCR1* (FC = 2.5, $P = 0.06$). In general, these genes function as important mediators of the inflammatory response.

We also observed eight significantly upregulated noncytokine/chemokine-related genes (**Table 1**). Several of the most significantly altered genes include the immune checkpoint proteins, *PDCD1* (PD-1, 18.9-fold) and *CD276* (B7H3; 1.75-fold). In addition, an increase was found in the interleukin receptors *IL2RB* and *CSF2RB*, as well as *PECAM1*, platelet endothelial cell adhesion molecule 1. Eight genes were significantly downregulated, including *CRTAM*, a cytotoxic and regulatory T-cell molecule that regulates the activation, differentiation, and tissue retention of T cells. *GZMA*, granzyme A, found in cytotoxic T lymphocytes was also reduced. Finally, there was a significant downregulation of *CDKN2A*, cyclin-dependent kinase inhibitor 2A that encodes p16 and is expressed in senescent cells.

PD-1 is the most upregulated gene

An immunofluorescence analysis was performed to determine the protein expression of PD-1 within the colon tissue. Its colocalization with CD8, a T-cell marker was also assessed (**Fig. 2B**). As shown in **Fig. 2C**, the numbers of PD-1^+–$CD8^+$ double-positive intraepithelial lymphocytes (IEL) were significantly increased within the ACF epithelia, accounting for approximately 2.82 ± 0.02 cells per 200 crypt cells. Interestingly, there were no double-positive cells detected within the stromal cells adjacent to the dysplastic crypts. Although there were significantly more PD-1^+ CD8 T cells in ACF, the overall number of CD8 cells in the stromal and epithelial compartments was reduced by approximately one third in ACF versus normal tissue (Supplementary Table S3).

Expression changes in the stromal compartment

To further investigate the differences between ACF and adjacent normal mucosa, we performed DGE on genes from the stromal compartment (**Fig. 2D**; Supplementary Figs. S2B and S4). We found six upregulated cytokine/chemokine genes in the stroma of ACF relative to normal mucosa (**Table 1**). These alterations are consistent

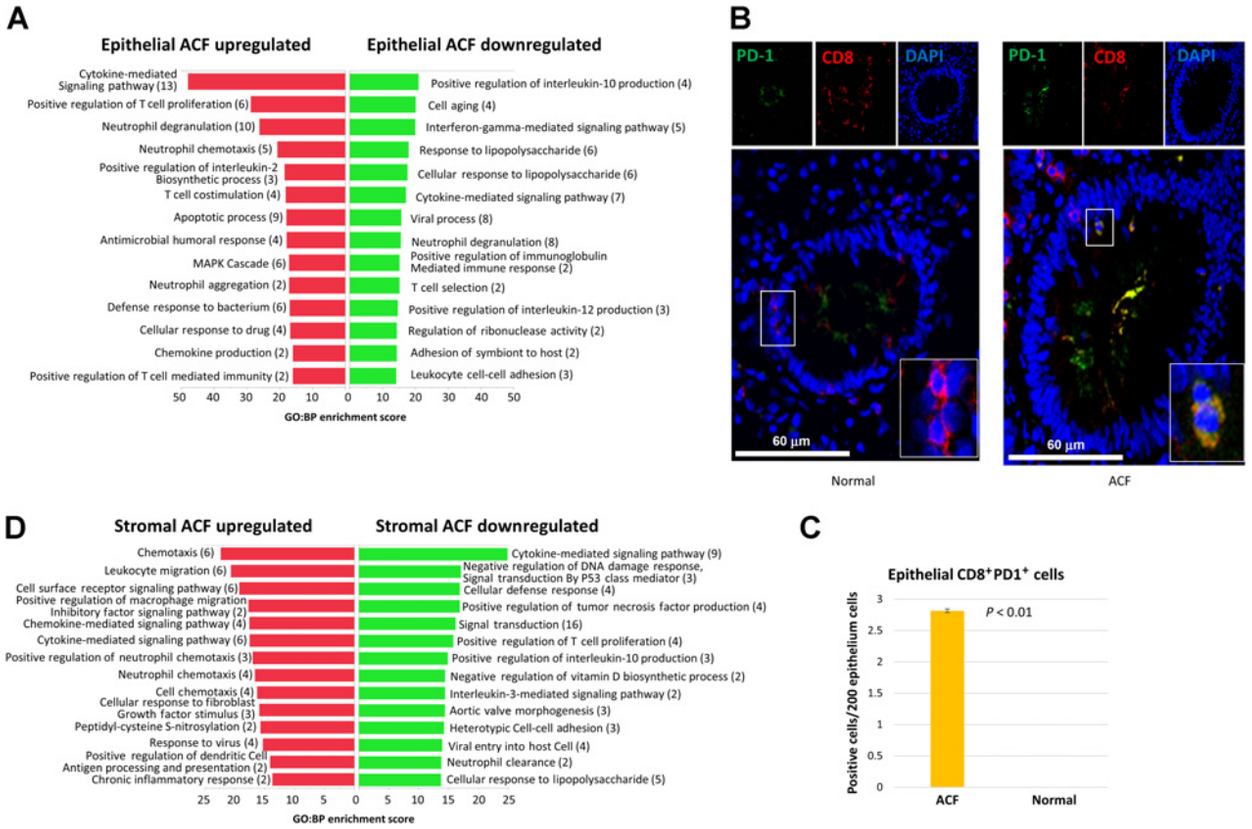

Figure 2.

Enriched GO:BP terms from epithelial and stromal samples revealed key biological processes. Immunofluorescence analysis of PD-1 and CD8 expression in normal and ACF mucosa. **A,** Enriched GO:BP terms from upregulated genes (left red) or down-regulated genes (right green) within the epithelial ACF dataset. Numbers in parenthesis indicate number of genes matched to each term. Enrichment score is a negative $\log_2$ representation of adjusted *P* value, all terms showing have adjusted *P* value < 0.0001. **B,** Colon biopsies were prepared for immunofluorescence staining as described under Materials and Methods. Representative immunofluorescence staining of PD-1 and CD8 in normal mucosa and ACF epithelium (20×). DAPI staining is used to outline cells. CD8 and PD-1 double-stained cells were observed on ACF. **C,** Quantification of double-positive cells ($n = 6$ samples/group). Two-sided Student *t* test is used to compare ACF and normal. **D,** Enriched GO:BP terms from upregulated genes (left red) or downregulated genes (right green) within the stromal ACF dataset.

with the results of the gene set analysis (**Fig. 2D**), in which the GO:BP score for "Cytokine-mediated Signaling Pathway" is at the top. Top genes include chemokines and chemokine receptors previously implicated in cancer (*CXCL13*, *CXCR4*, and *CCR7*; refs. 9–14). Upregulated *CCL22* is a macrophage-derived chemokine that binds to *CCR4* and can promote Treg recruitment to cancer tissue (15). Finally, *S100A8*, which encodes a calcium- and zinc-binding protein that regulates the inflammatory response, was also significantly increased. Also referred to as calprotectin, *S100A8* may play a role in myeloid-derived suppressor cell recruitment (16).

In **Table 1**, a set of noncytokine/chemokine-related genes that were significantly altered in either ACF stroma or epithelium are also listed. Surprisingly, the most elevated (16.9-fold; $P < 0.01$) stromal gene was *CDKN2A*, which was reduced in the ACF epithelial compartment. The number of selected downregulated genes present in the stroma was more extensive (**Table 1**), with nine genes achieving statistical significance and several more genes that were approaching significance. *TWIST1*, a regulator of transcription during organogenesis that plays a key role in tumor initiation and progression and *KLFR1*, an activating coreceptor expressed on the surface of NK cells, were both markedly reduced. *CMKLR1*, the receptor for chimerin that may play a role in regulating inflammatory responses within the tumor microenvironment, was also significantly reduced (10.0-fold). A variety of other genes involved in various aspects of inflammation and tumorigenesis were also reduced, including *GNLY* and *TBX21* (**Table 1**). *TBX21* encodes a Th1 cell transcription factor and *GNLY* is a CTL product, both pointing to a suppression in Th1 cell activity in the stroma of ACF.

Discussion

In our previous study describing molecular alterations associated with the earliest stages of human colon neoplasia, we applied an exquisitely sensitive technological approach to study diminutive ACF lesions that are common within the colonic mucosa (1). To expand upon these earlier findings, we performed an expression profiling analysis incorporating an expanded gene panel that includes a total of 395 immune-related gene targets, focusing on early dysplastic microlesions formed within the proximal (right) colon. Our results have uncovered a wide range of gene expression changes that accompany ACF formation, many of which may impact cancer promotion.

Many of the upregulated genes are consistent with neutrophil and macrophage chemotaxis and activation, including a number of chemokines and chemokine receptors. The activity of the chemokines in

Table 1. Fold change of representative genes that are altered in the epithelial or stromal compartment of ACF.

Type	Gene	FC in Epithelial	*P* in Epithelial	FC in Stromal	*P* in Stromal
Cytokine & chemokines	CXCL9	5.86	0.07	4.41	0.06
	S100A9	5.49	<0.01	1.15	0.77
	CXCL8	5.42	0.03	11.76	<0.01
	CXCL1	4.31	<0.01	1.63	0.06
	S100A8	3.32	<0.01	2.95	0.03
	CCR1	2.55	0.06	0.82	0.49
	CXCR4	0.49	0.16	5.52	<0.01
	CCL22	0.48	0.55	6.15	0.01
	HGF	0.28	<0.01	0.44	<0.01
	CXCL13	0.12	0.05	18.53	<0.01
	CCR7	0.01	<0.01	6.8	<0.01
Noncytokines	PDCD1	18.9	<0.01	1.7	0.35
	ALOX15B	4.02	<0.01	0.52	0.018
	NCF1	2.07	<0.01	0.71	0.17
	CSF2RB	1.96	<0.01	0.6	0.03
	IL2RB	1.82	<0.01	1.12	0.57
	KLRF1	1.81	0.82	0.01	<0.01
	PECAM1	1.8	0.05	0.64	0.17
	CD276	1.75	<0.01	0.84	0.31
	TBX21	1.54	0.25	0.62	0.04
	BST2	1.39	0.17	0.41	<0.01
	IFIT2	1.35	0.28	1.55	<0.01
	CD14	0.53	<0.01	0.49	<0.01
	GNLY	0.5	0.05	0.56	<0.01
	CMKLR1	0.41	0.42	0.1	<0.01
	TWIST1	0.38	0.42	0.01	<0.01
	CDKN2A	0.08	<0.01	16.99	0.01
	GZMA	0.06	<0.01	1.03	0.99
	CRTAM	0.01	<0.01	1.17	0.92

Note: Red highlighted boxes indicate those genes that are significantly upregulated in ACF epithelium relative to normal mucosa. Green highlighted boxes indicate those genes that are significantly downregulated. Uncolored boxes indicate those genes that are either significantly altered in another compartment, or have near-significant *P* values.

recruiting inflammatory cells is supported by the increased expression of the NADPH oxidase subunit *NCF1*. The ROS produced by this enzyme system can inflict oxidative DNA damage that may fuel lesion progression (17). Interestingly, *NCF1* is found in the epithelial compartment, in close proximity to the mutated epithelial cells. Also expressed within the epithelial compartment is the *PECAM1* adhesion molecule, which can be expressed by a range of different cell types (including transformed cells) and may play a role in adhering inflammatory cells in the epithelial compartment (18).

Another set of genes found to be differentially regulated in ACF relates to T-cell function. We found a striking elevation of *PDCD1* expression (~19-fold) within the epithelial compartment. *PDCD1* encodes the PD-1 receptor that is expressed on the surface of T cells and other hematopoietic cells (19). IF analysis showed PD-1 expression primarily on the surface of CD8 cells embedded within the epithelium. Although PD-1 is not sufficient for the induction of T-cell exhaustion, it is needed to maintain this cellular state, suggesting that the CD8 cells in ACF may be prone to checkpoint regulation (20). With regard to the PD-1 ligand PD-L1, RNA expression was observed within both ACF and normal crypts. Although PD-L1 was not (on average) increased in ACF, there was considerable variability in its expression. The expression of PD-L1 may be an important determinant of T-cell exhaustion in ACF and the risk of lesion progression. Other ACF changes are also consistent with suppressed T-cell function: a dramatic reduction of *CRTAM* expression, which encodes an adhesion molecule that promotes CD8 cell activation (21); an increase in *CCL22* expression, which functions as a Treg chemokine, and is often expressed by mature dendritic cells and macrophages in cancers (22, 23); and an increase in *S100A8* expression, which is expressed by premature myeloid cells to recruit immune-suppressing MDSCs (24). Overall, our findings raise the possibility that immunosurveillance is suppressed in these very early ACF lesions. Consistent with a reduced cytotoxic T-cell activity, expression of the effector genes *GZMA* (granzyme A) and *GNLY* (granulysin) were also reduced.

A biological process shown to be significantly altered in the ACF was "cell aging." Within this category is *CDKN2A*, which showed a 10-fold reduction in expression in the epithelium. *CDKN2A* encodes the CDK inhibitor, p16, which has cancer-suppressing activity. *CDKN2A* expression can be activated upon cell senescence, oncogene activation, and DNA damage (25). The decreased expression of *CDKN2A* in the epithelium is in contrast to the finding that this gene is frequently activated in colonic adenomas (26). It is possible that ACF have not yet reached critical thresholds of oncogenic signaling and/or telomere shortening to activate *CDKN2A*. Although p16-positive cells can be detected within ACF, our findings indicate that it is largely downregulated in these proximal lesions (27). In contrast to the epithelium, the stromal component of ACF showed a 17-fold increase in *CDKN2A* expression. *CDKN2A* activation in the stroma suggests that senescent fibroblasts may accumulate within ACF (28). Senescent cells accumulate with age, but can prematurely arise as a result of chronic inflammation and oxidative stress. They can also perpetuate an inflammatory microenvironment by acquiring a senescence-associated secretory phenotype (SASP), which is characterized by the increased expression of cytokines, chemokines, and tumor-promoting growth factors (29). However, more work is required to conclusively demonstrate their presence in the ACF (including an analysis of additional SASP markers) and to assess their impact on lesion progression.

In summary, we provide evidence that significant molecular alterations are present within the mucosa of early colonic neoplasia. ACF represent a very early stage of colonic neoplasia. Our results point to an acute inflammatory state present within proximal ACF lesions. In addition, PD-1 expression on T cells are elevated within the ACF epithelium, suggesting a suppression of immune surveillance. Our data suggest that these immunological changes may provide an accurate risk marker for progression risk, which could also help guide the development of intervention strategies to prevent lesion progression.

Authors' Disclosures

G. Lowman is a full-time employee of Thermo Fisher Scientific. No disclosures were reported by the other authors.

Authors' Contributions

T. Ideta: Conceptualization, formal analysis, investigation, visualization, writing–original draft, writing–review and editing. **B. Li:** Formal analysis, investigation, visualization, writing–original draft, writing–review and editing. **C. Flynn:** Investigation. **Y. Igarashi:** Investigation. **G. Lowman:** Resources, formal analysis. **T. Looney:** Resources, formal analysis. **T.J. Devers:** Resources, investigation. **J. Birk:** Resources. **F. Forouhar:** Resources. **C. Giardina:** Visualization, writing–review and editing. **D.W. Rosenberg:** Conceptualization, supervision, funding acquisition, project administration, writing–review and editing.

Acknowledgments

This work was supported by the State of Connecticut Department of Public Health (DPH) grant 2016-0092, NIH/NCI grants 1R01CA159976-01, 5R21CA231255, 5R03CA235225 (to D.W. Rosenberg), and a grant from the American Institute of Cancer Research/California Walnut Commission. This article is dedicated to Dr. Thomas J. Devers, a beloved colleague and friend who passed away on June 16, 2019. Without his unwavering dedication as a physician and scientist, this study would not have been possible.

Received March 29, 2021; revised August 12, 2021; accepted October 15, 2021; published first October 20, 2021.

References

1. Mo A, Jackson S, Varma K, Carpino A, Giardina C, Devers TJ, et al. Distinct transcriptional changes and epithelial-stromal interactions are altered in early-stage colon cancer development. Mol Cancer Res 2016;14:795–804.
2. Rosenberg DW, Yang S, Pleau DC, Greenspan EJ, Stevens RG, Rajan TV, et al. Mutations in BRAF and KRAS differentially distinguish serrated versus non-serrated hyperplastic aberrant crypt foci in humans. Cancer Res 2007;67:3551–4.
3. Drew DA, Mo A, Grady JJ, Stevens RG, Levine JB, Brenner BM, et al. Proximal aberrant crypt foci associate with synchronous neoplasia and are primed for neoplastic progression. Mol Cancer Res 2018;16:486–95.
4. Hanley MP, Hahn MA, Li AX, Wu X, Lin J, Wang J, et al. Genome-wide DNA methylation profiling reveals cancer-associated changes within early colonic neoplasia. Oncogene 2017;36:5035–44.
5. Drew DA, Devers TJ, O'Brien MJ, Horelik NA, Levine J, Rosenberg DW. HD chromoendoscopy coupled with DNA mass spectrometry profiling identifies somatic mutations in microdissected human proximal aberrant crypt foci. Mol Cancer Res 2014;12:823–9.
6. Hurlstone DP, Karajeh M, Sanders DS, Drew SK, Cross SS. Rectal aberrant crypt foci identified using high-magnification-chromoscopic colonoscopy: biomarkers for flat and depressed neoplasia. Am J Gastroenterol 2005;100:1283–9.
7. Inoue A, Okamoto K, Fujino Y, Nakagawa T, Muguruma N, Sannomiya K, et al. B-RAF mutation and accumulated gene methylation in aberrant crypt foci (ACF), sessile serrated adenoma/polyp (SSA/P) and cancer in SSA/P. Br J Cancer 2015;112:403–12.
8. Love MI, Huber W, Anders S. Moderated estimation of fold change and dispersion for RNA-seq data with DESeq2. Genome Biol 2014;15:550.
9. Hussain M, Adah D, Tariq M, Lu Y, Zhang J, Liu J. CXCL13/CXCR5 signaling axis in cancer. Life Sci 2019;227:175–86.
10. Kazanietz MG, Durando M, Cooke M. CXCL13 and its receptor CXCR5 in cancer: inflammation, immune response, and beyond. Front Endocrinol 2019;10:471.
11. Furusato B, Mohamed A, Uhlen M, Rhim JS. CXCR4 and cancer. Pathol Int 2010; 60:497–505.
12. Mburu YK, Wang J, Wood MA, Walker WH, Ferris RL. CCR7 mediates inflammation-associated tumor progression. Immunol Res 2006;36:61–72.
13. Xu B, Zhou M, Qiu W, Ye J, Feng Q. CCR7 mediates human breast cancer cell invasion, migration by inducing epithelial-mesenchymal transition and suppressing apoptosis through AKT pathway. Cancer Med 2017;6:1062–71.
14. Zhou W, Guo S, Liu M, Burow ME, Wang G. Targeting CXCL12/CXCR4 axis in tumor immunotherapy. Curr Med Chem 2019;26:3026–41.
15. Martinenaite E, Munir Ahmad S, Hansen M, Met O, Westergaard MW, Larsen SK, et al. CCL22-specific T cells: modulating the immunosuppressive tumor microenvironment. Oncoimmunology 2016;5:e1238541.
16. Deguchi A, Tomita T, Ohto U, Takemura K, Kitao A, Akashi-Takamura S, et al. Eritoran inhibits S100A8-mediated TLR4/MD-2 activation and tumor growth by changing the immune microenvironment. Oncogene 2016;35: 1445–56.
17. Irrazabal T, Thakur BK, Kang M, Malaise Y, Streutker C, Wong EOY, et al. Limiting oxidative DNA damage reduces microbe-induced colitis-associated colorectal cancer. Nat Commun 2020;11:1802.
18. Tang DG, Chen YQ, Newman PJ, Shi L, Gao X, Diglio CA, et al. Identification of PECAM-1 in solid tumor cells and its potential involvement in tumor cell adhesion to endothelium. J Biol Chem 1993;268:22883–94.
19. Keir ME, Butte MJ, Freeman GJ, Sharpe AH. PD-1 and its ligands in tolerance and immunity. Annu Rev Immunol 2008;26:677–704.
20. Hashimoto M, Kamphorst AO, Im SJ, Kissick HT, Pillai RN, Ramalingam SS, et al. CD8 T cell exhaustion in chronic infection and cancer: opportunities for interventions. Annu Rev Med 2018;69:301–18.
21. Cortez VS, Cervantes-Barragan L, Song C, Gilfillan S, McDonald KG, Tussiwand R, et al. CRTAM controls residency of gut CD4+CD8+ T cells in the steady state and maintenance of gut CD4+ Th17 during parasitic infection. J Exp Med 2014;211:623–33.
22. Rapp M, Wintergerst MWM, Kunz WG, Vetter VK, Knott MML, Lisowski D, et al. CCL22 controls immunity by promoting regulatory T cell communication with dendritic cells in lymph nodes. J Exp Med 2019;216:1170–81.
23. Rohrle N, Knott MML, Anz D. CCL22 signaling in the tumor environment. Adv Exp Med Biol 2020;1231:79–96.
24. Srikrishna G. S100A8 and S100A9: new insights into their roles in malignancy. J Innate Immun 2012;4:31–40.
25. Larsson LG. Oncogene- and tumor suppressor gene-mediated suppression of cellular senescence. Semin Cancer Biol 2011;21:367–76.
26. Kriegl L, Neumann J, Vieth M, Greten FR, Reu S, Jung A, et al. Up and downregulation of p16(Ink4a) expression in BRAF-mutated polyps/adenomas indicates a senescence barrier in the serrated route to colon cancer. Mod Pathol 2011;24:1015–22.
27. Dai CY, Furth EE, Mick R, Koh J, Takayama T, Niitsu Y, et al. p16(INK4a) expression begins early in human colon neoplasia and correlates inversely with markers of cell proliferation. Gastroenterology 2000;119:929–42.
28. Guo Y, Ayers JL, Carter KT, Wang T, Maden SK, Edmond D, et al. Senescence-associated tissue microenvironment promotes colon cancer formation through the secretory factor GDF15. Aging Cell 2019;18:e13013.
29. Kuilman T, Michaloglou C, Vredeveld LC, Douma S, van Doorn R, Desmet CJ, et al. Oncogene-induced senescence relayed by an interleukin-dependent inflammatory network. Cell 2008;133:1019–31.